Ecohydrology of a seasonal cloud forest in Dhofar: 2. Role of clouds, soil type, and rooting depth in tree-grass competition

Anke Hildebrandt[1,2] and Elfatih A. B. Eltahir[1]

Received 19 June 2006; revised 9 July 2007; accepted 24 July 2007; published 15 November 2007.

[1] Using a dynamic ecosystem model, we investigate the role of summer cloud immersion in the ecohydrology of a seasonal deciduous forest in Oman. This is a semiarid region where vegetation is immersed in dense cloud during a 3-month-long monsoon season. The simulated vegetation at equilibrium depends strongly on cloud cover during the wet season, with trees predicted under cloudy conditions and grasses when assuming a cloud-free monsoon. By varying soil type and rooting depth, we identify a rooting depth at which tree performance is optimal. This is the depth at which transpiration is maximized and the sum of all other fluxes from the soil is minimized. Our analysis shows that cloud cover creates a favorable seasonality in this ecosystem that is crucial for maintaining trees. This is achieved by (1) prolonging the growing season from 3 months to 6 months and (2) allowing deeper infiltration, which assures competitiveness of trees in an otherwise too dry environment.

Citation: Hildebrandt, A., and E. A. B. Eltahir (2007), Ecohydrology of a seasonal cloud forest in Dhofar: 2. Role of clouds, soil type, and rooting depth in tree-grass competition, *Water Resour. Res.*, *43*, W11411, doi:10.1029/2006WR005262.

1. Introduction

[2] In this research we are concerned with a water-limited ecosystem on the Arabian Peninsula (Governorate of Dhofar, Sultanate of Oman), where the rainy season is accompanied by sustained cloud immersion. On the basis of field measurements, we proposed in the companion paper [*Hildebrandt et al.*, 2007] that this forest could be considered a seasonal cloud forest, since clouds seem to be a necessary factor for survival of trees in this dry environment. The clouds reduced incoming radiation and atmospheric water demand. Transpiration was reduced during the cloudy monsoon and instead shifted to the following dry period. On the basis of sap velocity and soil moisture measurements we concluded that cloud shading reduced evapotranspiration and allowed for deep infiltration, despite precipitation being very limited. The soil storage was depleted only during the months following the cloudy season. The vegetation could be maintained as much as three more months after the end of the moist season. In this paper, we use a numerical model to investigate in more detail the influence of the seasonal cloud cover on the radiation budget and on expected vegetation structure. We vary radiation and soil environment and investigate the process by which the seasonal cloud cover favors trees in this semiarid climate through underground resource partitioning. While we describe a particular study site, our focus on a seasonal switch in cloud cover may be useful in examining other semiarid sites with favorable seasonality of precipitation.

[3] Access to water is a major determinant of plant survival in arid and semiarid ecosystems. Since plants lose water during photosynthetic assimilation, a limited water supply reduces carbon uptake and net primary productivity. Therefore, when moving on the globe from moist to drier climate zones, the vegetation also changes. It becomes less dense, and tall trees are replaced by smaller plants like shrubs and grassland [e.g., *Lieth and Whittaker*, 1975]. A number of climate vegetation charts are based on this observation [*Holdridge*, 1947; *Whittaker*, 1975]. Some relate expected vegetation to annual precipitation, temperature, potential evaporation, or lumped aridity indices. Traditionally, seasonality is not the main focus when evaluating potential vegetation, but observations suggest that seasonality plays an important role in setting water availability and vegetation distribution [*Brown et al.*, 1997; *Schenk and Jackson*, 2005; *Stephenson*, 1990]. For example, in regions with considerable rainfall during the cold season, deep infiltration is possible, and leads to a soil storage that deep rooted plants can at least partly use during the following warm season to alleviate water stress [*Ehleringer et al.*, 1991]. This mechanism is similar to resource partitioning between annual and perennial vegetation, first proposed by *Walter* [1962]. He suggested that trees and grasses coexisted in savannas as a result of below-ground niche separation for soil moisture, and they were therefore able to maintain high net primary productivity on minimal available water. The two-layer hypothesis has been shown to be applicable at some sites [*Sala et al.*, 1989; *Williams and Albertson*, 2004], but was rejected at others [*Scholes and Walker*, 1993]. However, climate seasonality may add a twist to *Walter*'s [1962] hypothesis [*Schwinning et al.*, 2002; *Stephenson*, 1990]. On the basis

[1] Department for Civil and Environmental Engineering, Massachusetts Institute of Technology, Cambridge, Massachusetts, USA.
[2] Now at UFZ Helmholtz Centre for Environmental Research, Leipzig, Germany.

0043-1397/07/2006WR005262$09.00

of observation of rooting depth in different environments, *Schenk and Jackson* [2002b, 2005] concluded that *Walter*'s [1962] hypothesis might be valid in ecosystems with a cold growing season, like those occurring in the Mediterranean. Other research indicated that niche separation is not rigid, but perennial plants are able to use water from deep soil storage from older winter rains, while they may amend or replace it with shallow, recently stored summer rain in case it becomes available [*Schwinning et al.*, 2002]. However, observations suggest that uptake depths increase under prolonged drought in environments where water was recharged in a previous season [*Romero-Saltos et al.*, 2005], which might eventually favor the most deeply rooted plants [*Schwinning et al.*, 2005].

[4] Over the forests of Dhofar, sustained cloud cover creates a cool climate during the growing season; creating an equivalent of a Mediterranean climate, where water can be stored in deep layers during the rainy season and used well past the last rains. Here, using a dynamic ecosystem model, we investigate how modification of radiation through clouds (and its seasonality) might influence potential vegetation and competition between trees and grasses in this semiarid environment.

2. Study Site

[5] The area of interest is a deciduous semiarid forest located in the southeast portion of the Sultanate of Oman within the coastal mountain range. The location and environment was described in detail in the companion paper [*Hildebrandt et al.*, 2007]. The climate is semiarid with a 3-month-long monsoon season (locally called khareef, mid-June to mid-September), which coincides with cloud immersion. In addition to rainfall, water droplets from the clouds collect on the foliage, such that total water received on the ground (net precipitation) exceeds rainfall. According to climate station data, more than three quarters of the annual rainfall falls during the monsoon, except for years when cyclones occur (return frequency of cyclones is only 1 in 2–4 years (a) [*Brook and Shen*, 2000]). The total net precipitation received during the monsoon was estimated as either 246 or 295 mm, depending on whether missing periods (14 days) were replaced with seasonal average (3 mm/d) or measurements from the directly preceding period. The latter better reflects the moister conditions during the time when the data loss occurred (beginning of the monsoon). 70% of net precipitation was throughfall and 30% stemflow, which appeared to increase infiltration in proximity of the tree trunks [*Hildebrandt et al.*, 2007]. During the rest of the year (mid-September to mid-June) the climate was desert like, with clear sky, high insolation, and high evaporative demand. However, the tree vegetation used water from soil storage for transpiration, thus the growing season ended early December in 2003 and end of December in 2004, 3 months after the end of the wet season.

3. Model Description

3.1. Original Model

[6] For this modeling study we used the integrated biosphere simulator (IBIS) [*Foley et al.*, 1996]. A detailed description of IBIS is given by *Foley et al.* [1996] and *Kucharik et al.* [2000]. Only the most important aspects are repeated here.

[7] IBIS is a dynamic ecosystem model combined with a surface vegetation atmosphere transfer (SVAT) scheme. The one-dimensional model is vertically organized in layers, including vegetation layers (upper and lower canopy) and a varying number of soil layers. The vegetation itself is differentiated into plant functional types (PFTs), which are described as either upper (trees) or lower (shrubs, herbs) canopy layer, and in addition differ in leaf form (conifers, broadleaf), leaf habit (deciduous, evergreen) and photosynthetic pathway (C3, C4). Each of the PFTs is assigned a number of physiological parameters and properties, such as rooting profile, the slope of the conductance-photosynthesis relationship, and allocation pattern of carbon within the plant [*Kucharik et al.*, 2000]. Throughout the simulation the PFTs compete with each other for two limited resources: light and water. Depending on the assigned vegetation properties, the success of securing those resources differs among PFTs and depends strongly on the environment. Nutrient availability is not considered in the present version of IBIS.

[8] During any IBIS simulation, a land surface module computes vertical water, energy, momentum and carbon fluxes on an hourly basis. Each day, the phenology module determines the state of deciduous and nondeciduous PFTs according to the season. At the end of the year the carbon balance module integrates the net plant carbon assimilation as the sum of photosynthesis and respiration, and computes the projected or one-sided leaf area index (LAI) as well as biomass for each PFT.

[9] The land surface module of IBIS calculates the amount of water (T_i) extracted from each layer (i = 1..n) as

$$T_i = T \cdot F_i, \tag{1}$$

where T is total transpiration and F_i is the root water uptake profile. IBIS calculates total transpiration in a separate module on the basis of theoretical turbulent exchange of water vapor with the atmosphere. As such transpiration depends in this model on atmospheric demand as well as stomatal conductance (which decreases when soil water is limiting; for more details, see *Foley et al.* [1996]). F_i is calculated on the basis of the fraction of root biomass (Y_i) and the water stress (W_i) in each layer:

$$F_i = \frac{Y_i W_i}{\sum_1^n Y_i W_i}. \tag{2}$$

The water stress (Wi) is a function of the soil water content. It ranges from 0 for no water uptake to 1 for unstressed uptake. Water stress also influences transpiration in IBIS, which is achieved by using the term

$$\xi_Y = \sum_1^n Y_i W_i \tag{3}$$

for scaling of stomatal conductance. Thus stomatal closure depends among others on soil water status and root distribution. The fraction of root biomass in each layer is

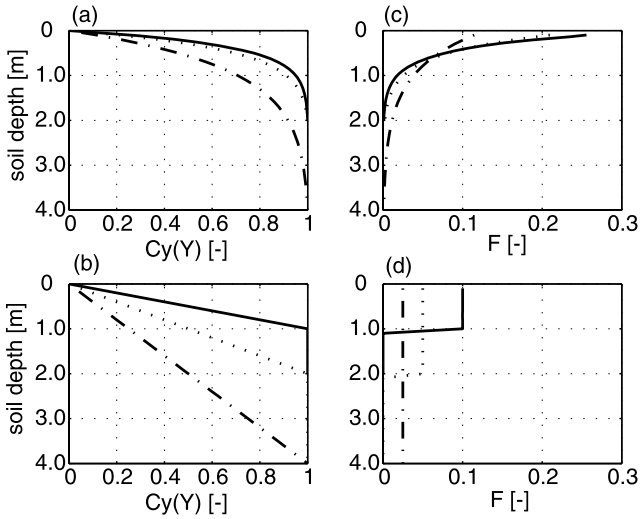

Figure 1. (left) Rooting density function and (right) corresponding water uptake profiles plotted for grass and trees with two different rooting depths (2 m and 4 m) (a, c) for parameterization of *Gale and Grigal* [1987], with β = 0.72 for tropical grassland/savannah [*Jackson et al.*, 1997], β = 0.977 for 2.0 m deep rooted trees, and β = 0.988 for 4.0 m deep rooted trees, and (b, d) simple assumptions used for this research and rooting depth for grasses 1.0 m. In all plots, the solid line represents grasses, the dotted lines represent trees with 2.0 m rooting depth, and the dash-dotted lines represent trees with 4.0 m rooting depth, representing shallow and deeper-rooted trees. For the parameterization of Gale and Grigal we defined the rooting depth as the depth above which 99% percent of the root biomass is located.

found from the rooting profile $C_y(Y)$, which is described as a cumulative distribution function [*Gale and Grigal* [1987],

$$C_Y(Y) = 1 - \beta^d, \tag{4}$$

and indicates what percentage of the total root biomass is located above a given soil depth, d. $C_Y(Y)$ ranges from 0 at the surface to 1 at the maximum rooting depth. The shape parameter β was adopted from observation of root systems in different parts of the world and various ecosystems [*Jackson et al.*, 1996, 1997]. β has values close to one, with higher values leading to deeper roots.

3.2. Model Developments

[10] For this study we changed the parameterization of root water uptake profile (F_i). Equation (2) was developed on the basis of the assumption that water stress and root abundance determine how much water can be taken up from a given soil layer. According to equation (2), total transpiration decreases significantly when the upper soil layers (with high root abundance) dry out, while uptake from deeper soil layers is inhibited by low root fraction. In contrast, a number of observational studies suggest that plants are able to compensate with deep-water uptake, when shallow soil is dry [*Green and Clothier*, 1995; *Lai and Katul*, 2000; *Li et al.*, 2002]. One reason for this disagreement might be that equation (2) inherently states that it is not root abundance (for example expressed in root biomass per volume) that determines the root water uptake profile, but the fraction of roots in each soil layer, compared to total root biomass. However, while only a small fraction of the root system might be located in deep soil, those roots may be able to deliver a disproportionally large portion of water to the leaves. Under favorable conditions, wet parts of the root system seem to compensate for dry parts in order to maintain appropriate transpiration levels [*Green and Clothier*, 1995; *Sakuratani et al.*, 1999]. Overall, little experimental evidence exists on how root density is related to water extraction from the soil [*Wang and Smith*, 2004]. Furthermore, it has been shown that the same plant species can exhibit shallow or deep root distribution, likely as an adaptation to particular environments [*Hacke et al.*, 2000; *Lehmann*, 2003; *Wan et al.*, 2002]. Acknowledging the observed flexibility of plants to adjust their water uptake to changing environmental conditions, a workshop held on the representation of water uptake in SVAT schemes recommended to keep "root water uptake models as simple as possible, with an implicit description of roots that assumes that water in the root zone is available to the plants" [*Feddes et al.*, 2001, p. 2806]. Inappropriate representation of root water uptake has prompted other researchers to modify water uptake profiles in some SVAT schemes [*Kleidon and Heimann*, 1998], including a formulation for deep-water uptake compensation implemented in IBIS for a research project in Africa [*Li et al.*, 2005]. In the spirit of *Feddes et al.* [2001], and given the general lack of process understanding about root water uptake profiles, we changed equation (2) such that roots could take up water equally at any depth, independent of rooting density:

$$F_i = \begin{cases} 0 & \text{if } \sum_1^n W_i = 0 \\ \dfrac{d_i W_i}{\sum_1^n d_i W_i} & \text{otherwise,} \end{cases} \tag{5}$$

where d_i is the thickness of layer i, and n the total number of rooted layers. The equivalent term to equation (3) becomes

$$\xi_d = \sum_1^n d_i W_i. \tag{6}$$

The change also greatly simplifies interpretation and intuitive presentation of the following sensitivity study. Figure 1 illustrates the difference between the original and new parameterization.

4. Model Input

[11] IBIS requires two different types of input data: descriptions of the geographic location, vegetation and soil, and a time series of atmospheric boundary conditions (air temperature, precipitation, specific humidity, wind speed and cloudiness). For meteorological input we used the data measured at a field site (Gogub) [*Hildebrandt et al.*, 2007]. For all input except cloudiness we used the meteorological data from a single year and repeated it for 500 a. The time series used in all following model experiments starts 1 September 2003 and ends 31 August 2004. Missing data in the measured time series were replaced with values from

Table 1. Overview of the Model Analysis Conducted

Scenario	Boundary Condition	Soil Depth, m	Soil Type	Cloud Cover	IBIS Cloudiness Factor
RCC1	free drainage	3.0	sandy loam	cloudy khareef	*FC* = 1.0 15 Jun to 15 Sep 15; *FC* = 0.0 rest of the year
RCC2	free drainage	3.0	sandy loam	clear sky	*FC* = 0.0 all year
ERD1 C	free drainage	varied from 0.5 to 6.0	clay loam, sandy loam, sand	cloudy khareef	*FC* = 1.0 15 Jun to 15 Sep 15; *FC* = 0.0 rest of the year
ERD0 C	no flow	varied from 0.5 to 6.0	clay loam, sandy loam, sand	cloudy khareef	*FC* = 1.0 15 Jun to 15 Sep; *FC* = 0.0 rest of the year
ERD1 PC	free drainage	varied from 0.5 to 6.0	clay loam, sandy loam, sand	partial cloudy khareef	*FC* = 0.5 15 Jun to 15 Sep; *FC* = 0.0 rest of the year

the immediately preceding period. The longest such period is two weeks. The input for cloudiness used in IBIS is not the same as β in the companion paper [*Hildebrandt et al.*, 2007, equation (10)]. In IBIS, cloudiness (*CF*) is used to calculate the transmissivity of the atmosphere to several components of incoming shortwave radiation (visible and near infrared, diffuse and direct beam). *CF* varies from 0 to 1 with higher values decreasing atmospheric transmissivity. When calculating total incoming shortwave radiation for Dhofar using $CF = 1$, the values are similar to those observed during the monsoon, with a tendency to overestimate incoming shortwave radiation on days with strong cloud immersion, and the opposite for days with less cloud immersion. For clear days the fit is very good. As a first-order approximation we therefore represent cloud conditions in Dhofar with $CF = 1$ (cloudy) for the entire monsoon (15 June to 15 September), and $CF = 0$ (clear sky) at any other time of the year (unless otherwise stated).

[12] Instead of rainfall we used observed below canopy precipitation as water input, which better reflects plant available water, as it includes both rainfall and water captured from clouds. Stemflow (the volume of water running down the stem) is a point source of infiltration and leads to spatially variable water input at the soil surface [*Pressland*, 1976]. IBIS is a one-dimensional model that cannot account for point fluxes; instead it requires a uniform precipitation input in mm per time. We therefore convert stemflow volume to stemflow depth by isolating a likely infiltration area. Pressland showed that stemflow led to substantially elevated soil moisture within at a distance of 0.5 m around the stems, compared to 2.0 m. We chose a circle with radius of 0.75 as area of stemflow infiltration. Total infiltration around the stems during the khareef thus becomes 400 mm, rather than 295 mm had stemflow been distributed uniformly over the surface. Strictly speaking, this input applies only to the area around tree stems, which may overestimate the precipitation for grass.

[13] Since the khareef delivers the only reliable and recurring precipitation every year, we assumed that plants survive only on monsoon rain. We therefore omitted from the measured time series any occasional events that happened outside of the monsoon season. Most notably we did not include the rainfall from a cyclone that passed through the region in September 2004. Cyclones are rare in this region, with return frequency of only once every 2–4 a [*Brook and Shen*, 2000]. Moreover, soil moisture measurements showed that the cyclone of 2004 only influenced the upper soil layers. Recharge to the deeper layers was less than that from the monsoon [*Hildebrandt et al.*, 2007]. We therefore concluded that vegetation should be able to survive on monsoon precipitation alone. The other omitted events (total 4) were of negligible magnitude (<1 mm rainfall).

5. Analysis

[14] We performed a sensitivity analysis on the influence of cloud cover and soil environment on the vegetation type and hydrology of the seasonal cloud forest in Oman. All scenarios are summarized in Table 1.

[15] First, we investigated the role of cloud shading during the monsoon on vegetation structure by comparing model experiments where cloud cover during the monsoon is present (scenario RCC1: cloudy during the monsoon, clear sky during the rest of the year), with experiments where cloud cover during the monsoon is removed (scenario RCC2: clear sky all year round). All other input, including precipitation, is kept the same. Although this model is purely theoretical, it is illustrative to consider the role of cloud shading separately from precipitation, as will become clear below.

[16] Second, we investigated the influence of soil type and rooting depth on the vegetation structure. This investigation highlights the role of deep infiltration and below ground resource partitioning for competitiveness of trees in this environment. The soil type, depth and the lower boundary condition (free drainage or impermeable) were varied. The maximum rooting depth for grasses was set to one meter and for trees it was set equal to the assumed soil depth. When the soil depth was equal or smaller than one meter, the rooting depths of trees and grasses were the same (both defined by the soil depth). The lower boundary condition was either assumed to be free gravitational drainage (scenario ERD1 C) or impermeable (scenario ERD0 C), as indicated.

[17] Third, in order to gain insight into the influence of cloud cover on below ground resource partitioning and thus vegetation structure, we repeated the same experiments but reduced the cloudiness during the monsoon to partly closed cloud cover ($CF = 0.5$, scenario ERD1 PC) and compared the results.

[18] All model experiments were performed by repeating the model input (1 a) for 500 a, after which time equilibrium had been reached in all cases. Net primary productivity and the water fluxes are at equilibrium when they show no trend, though they fluctuate about a long-term mean. For initial vegetation we assumed both deciduous broadleaf tree and grassland. Initial vegetation had no influence on the model equilibrium. The predictions of the year 500 are

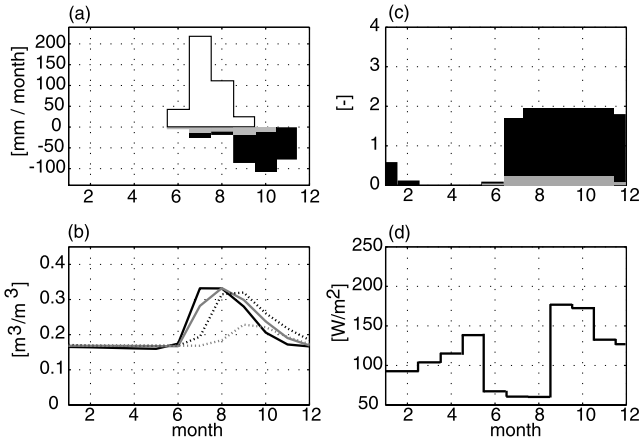

Figure 2. Model output for control simulation of expected conditions in Gogub (scenario RCC1): (a) monthly accumulated water budget, transpiration (black), soil evaporation (gray), and precipitation forcing (white); (b) monthly average volumetric soil water content, layers centered at 0.17 m (solid black line), 0.75 m (solid gray line), 1.5 m (dotted black line), and 2.5 m (dotted gray line); (c) monthly leaf area indices for upper (black) and lower (gray) canopy; and (d) monthly average net radiation. Note that the dotted lines in Figure 2b show the soil layers that are beyond the reach of grass.

presented as results, representing equilibrium conditions. Performance of tree and grass canopy is indicated by means of their LAI at equilibrium.

6. Modeling Results

6.1. Role of Cloud Cover in Decreasing Incoming Radiation

[19] In order to investigate the role of cloud cover in reducing incoming radiation during the monsoon, we first forced the model with observed climate, cloudy monsoon ($CF = 1$), while clear sky ($CF = 0$) was assumed for the rest of the year (scenario RCC1). The soil is a 3 m deep sandy loam.

[20] The resulting vegetation in this scenario is dominated by deciduous trees consistent with vegetation found at the field site. The monthly water budget, soil moisture, LAI and net radiation for scenario RCC1 are plotted in Figure 2. The results compare well with the observations at the field site (data not shown). Net radiation (Figure 2d) is strongly reduced during the khareef, therefore limiting the total amount of energy available for evapotranspiration. As a result, transpiration remains low during the khareef season (as observation suggested [*Hildebrandt et al.*, 2007]), reaches a maximum just after the end of the khareef in September and October, then declines steadily, eventually reaching values close to zero in January (Figure 2a). Similar to transpiration, direct soil evaporation is suppressed during the khareef. However, since the topsoil layer dries out quickly, evaporation does not reach a maximum after the khareef.

[21] Soil storage is filled during the moist season, and emptied during the month after the monsoon (Figure 2b). The upper four layers in Figure 2b (solid lines) match the measurement depths for soil moisture at the field experiment [*Hildebrandt et al.*, 2007]. Figure 3 compares modeled soil moisture with measurements made at the field site in the year 2004. To compare we normalized the model values in the same fashion as the measurements (see section 4.8 of *Hildebrandt et al.* [2007] for details) as

$$SM* = \frac{F_n - F_{\min}}{F_{\max} - F_{\min}}, \tag{7}$$

where $SM*$, is normalized soil moisture, $F_{\max}$ and $F_{\min}$ are the maximum and minimum observed (or modeled) values for soil moisture and F_n is the current observation. Examination of Figure 3 shows model prediction and field observation match well. An exception is the increase of soil moisture at the field site as a result of heavy rainfall from a cyclone in September 2004 which was omitted from the model input.

[22] The second scenario (RCC2) shows the importance of cloud shading during the monsoon. Here, we assumed clear sky ($CF = 0$) for the entire year. Note that the only difference between RCC2 and RCC1 is in the removal of cloud cover during khareef, and the resulting increase in incoming radiation. All other environmental conditions, such as precipitation, temperature and even the high relative humidity during the monsoon, were kept the same. The results are summarized in Figure 4. What is most striking is that the dominant vegetation is C4 grass, rather than trees as in RCC1. With cloud cover absent, the maximum of available energy is now shifted to July and August (Figure 4d). Most energy is thus available for evapotranspiration at the same time of year when precipitation occurs.

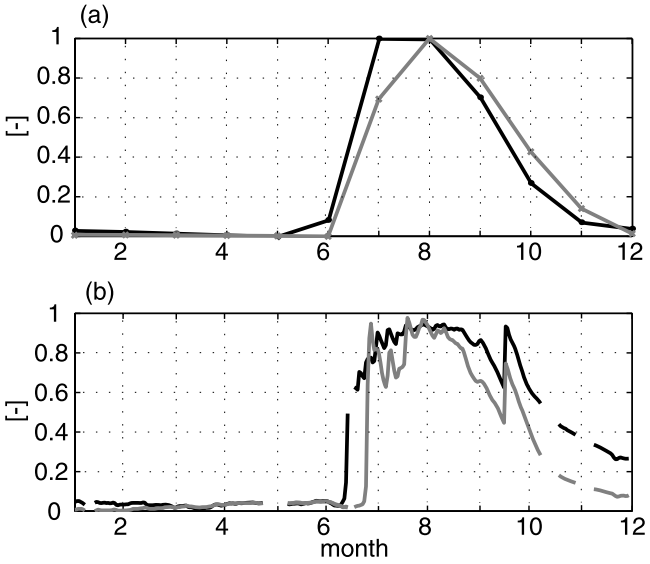

Figure 3. Soil moisture expressed as referenced value SM* (equation (7)). (a) Prediction from IBIS simulation for expected conditions in Gogub (scenario RCC 1). Layers are centered at depths 0.17 (black line) and 0.75 m (gray line). (b) Measured values in Gogub (January through December 2004); layers are centered at depths 0.15 (black line) and 0.55 m (gray line).

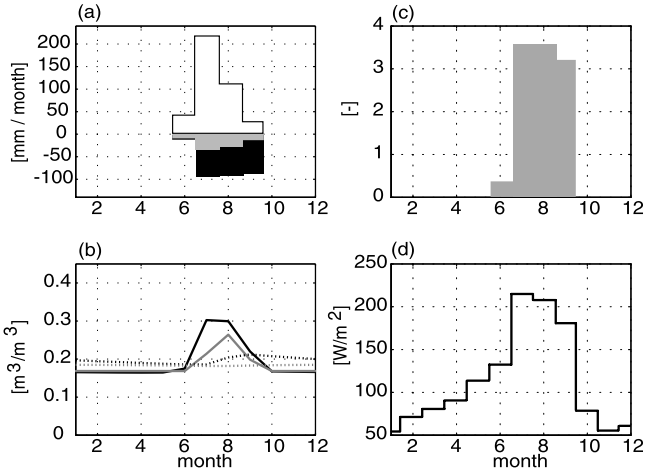

Figure 4. Same as Figure 2 except that clear sky was assumed all year round (scenario RCC2): (a) monthly accumulated water budget, transpiration (black), soil evaporation (gray), and precipitation forcing (white); (b) monthly average volumetric soil water content, layers centered at 0.17 (solid black line), 0.75 (solid gray line), 1.5 (dotted black line), and 2.5 m (dotted gray line); (c) monthly leaf area indices for the upper (not visible because LAI is zero) and lower (gray) canopy; and (d) monthly average net radiation.

As a result, water is removed from the upper soil layers by both transpiration and evaporation during the wet season itself (Figure 4b), keeping the water content in the upper soil layers low, and allowing little water to infiltrate to the lower layers. The water content of the lower layers is somewhat higher than in the upper ones, because the grass roots only reach 1.0 m depth and cannot make use of the water in the lower layers for transpiration. However, there is insufficient water to accommodate trees, although some water is stored for a long time in deep layers.

[23] In summary, the cloud cover in RCC1 pushes the transpiration peak later in the year, outside of the moist season. This corresponds to the canopy development during the same time, expressed in LAI. In the first case (RCC1), trees dominate the vegetation. They grow during the monsoon and have leaves until December, long after the last rain (Figure 2c). In the clear sky scenario RCC2 the vegetation is dominated by grasses, which are in leaf only during the monsoon and die off as soon as the rain period is over, leading to a growing season of only 3 months (Figure 4c).

[24] In RCC2, soil moisture is generally lower and there is little deep infiltration, although the same amount of water entered the soil as in RCC1. When clouds are present during the khareef, soil infiltration is deeper because of low evaporative demand and water is stored in the lower layers, where it is protected from soil evaporation and out of the reach of shallow-rooted plants (grass). This water is available for transpiration by deep-rooted plants (trees), during the period of high evaporative demand after the khareef. Modeled annual transpiration is 343 mm (85% of precipitation) in RCC1 and 287 mm (71% of precipitation) in RCC2. The difference is accounted for by change in direct soil evaporation.

6.2. Role of the Soil Environment and Optimum Rooting Depth

[25] The prolonged growing season as illustrated in the previous section would not be possible without sufficient water storage, where water is kept from one season to the next. The size of the storage is influenced by factors such as soil type, soil depth and the type of underlying rock (impermeable or conductive), which all vary greatly in the field. It is therefore valuable to investigate what influence the soil properties have on the vegetation performance in our model.

[26] An important property of soil is the water release curve, which defines both plant available soil storage and how hydraulic conductivity decreases as the soil dries. In all soils, the permanent wilting point is located at hydraulic conductivities that allow only negligible vertical water flow in the soil. This is true even for highly conductive soils such as sand. Thus, when the soil dries out, transpiration likely becomes more significant than drainage in removing water from a given soil volume. In semiarid environments this helps roots capture much of the water before it can flow out of their reach (it also allows for relatively long storage times). Once infiltrating water has percolated below the rooting zone the water is "lost" from the perspective of plants. We expect that plants in a water-limited ecosystem would adjust to make use of most of the infiltrating water and therefore have a rooting depth that enables them to capture as much water as possible. Since water retention (and therefore infiltration rate) depends on the soil type, plants may show a different rooting behavior in different soils.

[27] In the following we conducted a sensitivity analysis, where we varied soil type, soil depth (and with it rooting depth, as described in section 3), and the nature of the lower boundary condition (no drainage and free drainage). For all cases we evaluated the performance of the vegetation by comparing LAI at equilibrium. We were particularly interested in the performance of trees in this environment, so LAI of the upper and lower canopy separately.

[28] First, we consider the cases where the lower boundary condition is free drainage (ERD1 C). Figure 5a shows the LAIs of the upper (trees) and lower (grass) canopy at model equilibrium for varying soil depths in a sandy loam. The PFTs are drought deciduous tress and C4 grasses for the upper and lower canopy respectively for all simulated depths. The modeled tree LAIs show a distinct maximum at a soil depth of 2.75 m.

[29] The increase of LAI with soil depth can be explained by considering the water balance. The corresponding water budget (expressed in annual accumulated fluxes in mm) is plotted in Figure 5b. When rooting depths are shallow, a lot of water is lost through deep drainage. As rooting depth increases, more water can be captured by plants and is available for transpiration, net primary productivity, and hence for investment in LAI. The LAIs reach their maximum values at a critical depth where drainage ceases or is inconsequential small. Note that below this critical depth the lower boundary condition no longer matters because no water percolates downward. In other words, in this model the optimum condition occurs for the shallowest soil depth at which tree transpiration is maximized, and the sum of the other losses (e.g., drainage) are minimized.

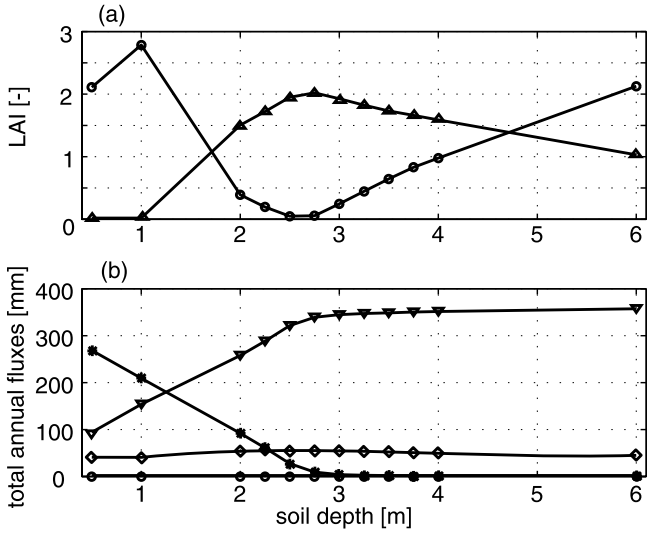

Figure 5. Predicted conditions at the end of a 500-a simulation with free drainage and cloudy khareef (scenario ERD1 C) for sandy loam and varying soil depth. (a) LAI for upper (deciduous trees, triangles) and lower canopy (C4 grass, circles) and (b) corresponding water budget for the same case, expressed in annual fluxes: transpiration (triangles), drainage (asterisks), evaporation (diamonds), and surface runoff (circles).

[30] As soil depth increases beyond the critical depth, tree LAIs decrease, and grass becomes more competitive. This trend is a result of the model parameterization for root water uptake. As stated in equation (5), the water uptake profile is spread uniformly across the root zone, which is assumed coincident with the soil depth for trees. At the same time, water stress affects transpiration as described in equation (6). Thus, when water uptake is stretched further across the soil profile, and uptake at a given depth must decrease. In other words, in order to reach deeper, trees sacrifice water uptake in the upper soil layers. Grass, with shorter uptake profile, has a higher uptake capacity in the upper soil layers and achieves overall higher uptake rates than trees with deeper than optimal rooting depth.

[31] In nature we would not expect trees to attempt water uptake beyond their optimum depth. Plants would likely attempt to keep roots as short as possible, for a number of reasons: (1) shallow root biomass is physiologically cheaper to maintain (2) shallow root soil layers are usually better aerated and (3) nutrient concentrations are often higher in shallow layers [*Schenk and Jackson*, 2002b]. Therefore it is reasonable to assume that we would find roots down to an efficient depth, even if the soil were deeper. The trend of decreasing tree LAI with increasing rooting depth found here is therefore a purely theoretical modeling result.

[32] The point of optimum tree performance in this model, or efficient depth, depends on the soil type. Figure 6a shows tree and grass LAI at equilibrium for different modeled rooting depths. The modeled optimum depth for clay loam is 2.25 m, for sandy loam at 2.75 m and for sand at 3.25 m (however, the focus here is not on the absolute modeled values, but on the general trend that they reflect). Figures 6b and 6c show the annual drainage and transpiration for the modeled soil types as a function of rooting depth. For heavy soils (with low infiltration rates) all available water can be removed with roots concentrated in shallow layers. For lighter soils (with faster infiltration),

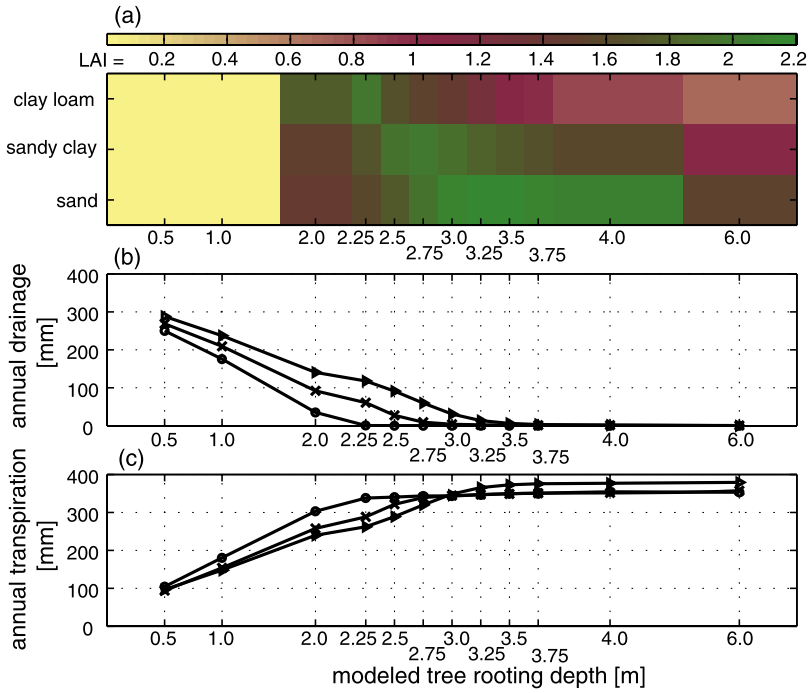

Figure 6. Overview over predicted conditions at the end of a 500-a simulation for scenario ERD1 C. (a) Predicted LAI of the upper canopy (deciduous trees), (b) corresponding total annual drainage, and (c) corresponding total annual transpiration. Soil types are sand (circles), sandy loam (crosses), and clay loam (triangles).

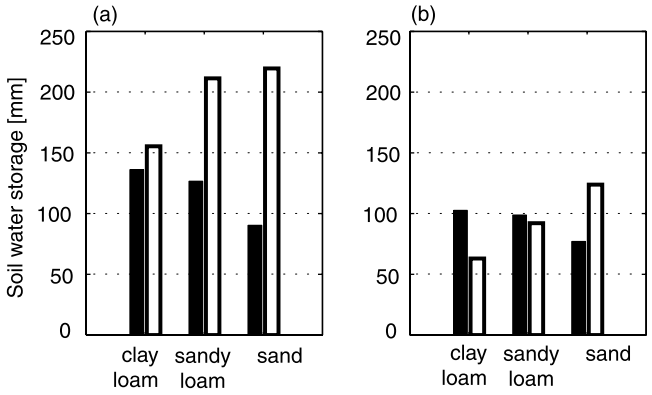

Figure 7. Difference between the monthly average soil storage in May (lowest soil storage before the khareef) and September (soil storage at end of khareef) at model equilibrium. Presented are the simulations at the respective optimum rooting depth. The storage is partitioned between the upper soil column (black, 0–1.0 m, accessible equally to trees and grasses) and the storage below 1 m (white, >1.0 m, storage accessible only to trees). (a) Cloudy monsoon (scenario ERD1 C) during the khareef; simulations at optimum rooting depth for clay loam (black, 0–1 m; white, 1–2.25 m), sandy loam (black, 0–1 m; white, 1–2.75 m), and sand (black, 0–1 m; white, 1–3.25 m). (b) Partly cloudy monsoon (scenario ERD1 PC); experiments at optimum rooting depth for clay loam (black, 0–1 m; white, 1–1.75 m), sandy loam (black, 0–1 m; white 1–2 m), and sand (black, 0–1 m; white, 1–2.25 m).

roots have to reach deeper in order to take advantage of the available water.

[33] The maximum LAI is higher in coarse soils than in fine soils, which is related to the fact that water is stored deeper when the soil is coarser. For the optimal rooting depths, the difference in soil storage between the average in May (lowest soil storage before the khareef starts) and September (at the end of the khareef) is shown in Figure 7a and results are summarized in Table 2. This difference illustrates how much water could be stored in the ground during the khareef, Table 2 also indicates what fraction of total khareef precipitation this increase in soil storage corresponds to. The storage for the shallow soil layers (0–1.0 m, the storage accessible to both trees and grasses) and deeper soil layers (>1.0 m, only accessible to trees) are also given separately. It is notable that trees were more competitive in coarse than medium textured soil, although the medium textured soil stored overall more water (compare columns 2 and 4 in Table 2). The explanation gives the partitioning of soil storage between the upper and lower soil layers, which is greater in sand (only one third of water is stored in the upper and two thirds are stored in the lower layers) than in finer soil (the upper and lower storage are nearly same in clay loam). As a result, the deep water storage that is only accessible to trees is greater in coarse than fine soil (Figure 7a), and consequently trees with optimal rooting depth compete better in coarse than fine soils.

[34] The same sensitivity analysis based on free drainage boundary condition can be reproduced for a no-flow boundary (ERD0 C), leading to similar results. The equilibrium LAIs for sandy loam are plotted in Figure 8a. Tree LAI first increases with increasing soil depth, reaching a maximum between 1.25–2.75 m rooting depth before decreasing. The reason for this behavior can again be found in the water balance (Figure 8b). Drainage is set to zero, and soil evaporation is more or less constant regardless of modeled soil depth. Surface runoff and transpiration are the variable fluxes. When the impermeable boundary layer is close to the surface, pore water content is elevated as compared to the free drainage scenario. Consequently, the infiltration capacity of the soil is reduced, and surface runoff occurs. The surface runoff is a loss term in the water balance and is therefore not available for transpiration. As a result tree LAI decreases in response to lower infiltration. In this scenario the critical rooting depth is the depth at which soil storage is large enough to allow for all water to infiltrate and surface runoff becomes zero.

[35] When the rooting depth is further increased beyond the efficient depth (in this example 1.25 m), LAI remains elevated until about 2.75 m. Recall that 2.75 m was the optimum rooting depth, i.e., the depth at which drainage ceased, for the same soil in the previous case (free drainage scenario, compare Figure 5). Thus between 1.25 and 2.75 m in this simulation the impermeable boundary is located between two points: the one where surface runoff ceases and the one where drainage would cease. Within this range LAI remains high and decreases only slowly. Beyond 2.75 m

Table 2. Summary of Results for Scenarios With Free Drainage, Optimum Depths, Corresponding LAI of Upper (Trees) and Lower (Grass) Canopy and Increase of Soil Storage Between the Beginning (June) and End (September) of the Khareef

Soil	Optimum Depth, m	LAI Trees	LAI Grass	Difference Between Soil Storage in June and September, mm	Part of Total Khareef Precipitation,[a] %	Part in Shallow Storage Available for Trees and Grasses Above 1 m, %	Part in Deep Storage Available for Trees Only Below 1 m, %
				Scenario ERD1 C			
Clay loam	2.25	1.95	0.10	291	72	47	53
Sandy loam	2.75	2.00	0.05	338	84	37	63
Sand	3.25	2.20	0.05	310	77	29	71
				Scenario ERD1 PC			
Clay loam	1.75	0.80	3.00	166	41	62	38
Sandy loam	2.00	1.45	1.30	191	47	52	48
Sand	2.25	1.70	1.15	201	50	38	62

[a]Total precipitation is 400 mm.

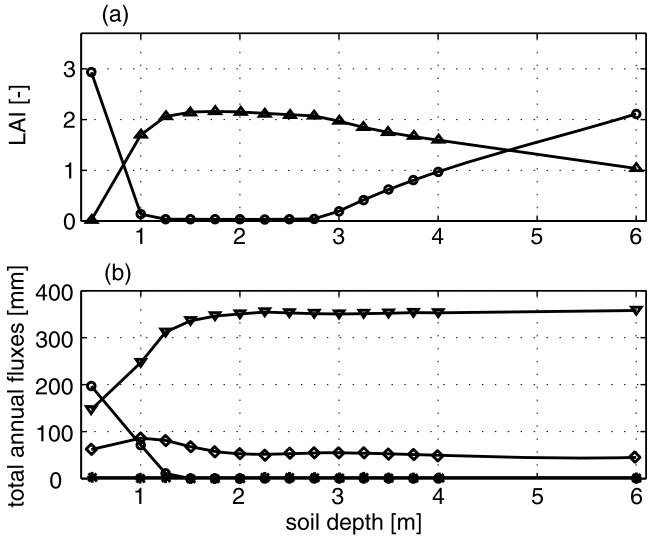

Figure 8. Predicted conditions at the end of a 500-a simulation with no drainage (scenario ERD0 C) for sandy loam and varying soil depth. (a) LAI for upper (deciduous trees, triangles) and lower (C4 grass, circles) canopy and (b) corresponding water budget for the same case, expressed in annual fluxes: transpiration (triangles), drainage (asterisks), evaporation (diamonds), and surface runoff (circles).

the boundary condition is irrelevant, since no more water is available to flow out of the lower boundary. Once this point has been reached we expect to find the same modeling results independent of assumed boundary condition. Comparison of Figures 5 and 8 confirms that this is indeed the case.

[36] Clearly, this scenario does not take into account the fact that soil layers would be highly saturated during the khareef, if the impermeable layer were found at the "optimum" level for water uptake. In fact, the soils would be water logged. Water logging has several negative effects on vegetation, such as low aeration, low biologic activity of the soil, and low availability of nutrients. We would therefore not expect trees to survive in an environment strictly at an efficient soil depths for water uptake, but at a depth lower than this. In this case the optimum rooting depth depends not only on water uptake but other environmental factors as well.

6.3. Role of Cloud Cover in Increasing the Competitiveness of Trees Versus Grasses

[37] We showed above that the radiative properties of the cloud cover in Dhofar facilitated effective filling of the soil storage during the khareef season. The following model experiments were performed to investigate the relation between cloud cover and rooting depth. For these experiments (scenarios ERD1 PC), we reduced cloud cover during the entire khareef season from $CF = 1$ (which reflected realistic incoming radiation) to $CF = 0.5$ (partly cloudy). This assumption leads to increased net radiation, higher canopy temperatures and higher evaporative demand, while precipitation is kept the same. The experiment was only performed for free drainage boundary condition.

[38] The LAIs and water budget for sandy loam are plotted in Figure 9. The summary for all soil types considered is plotted in Figure 10. As compared to the prediction for the same soil with $CF = 1$ (compare with scenario ERD1 C, Figure 5) the optimum depths have moved upward for each of the modeled soil types. For clay loam, the difference is 0.5 m, for the sandy loam 0.75 m and for sand 1.0 m. It is notable that the decrease in cloud cover had only a minor impact on direct soil evaporation, which was slightly increased (approximately 10–20 mm for all simulations).

[39] The reason for the upward shift of the optimum rooting depths is the higher evaporative demand during the khareef season. Water is now removed from the upper soil layers at the same time as they are recharged. As a result, less water percolates to the lower layers, the infiltration depths are decreased, and it is consequently more profitable for trees to take up water from more shallow depths. Figure 7b shows the difference in soil storage between the average in May (lowest soil storage, before the khareef starts) and September (at the end of the khareef), partitioned between the upper layers (0–1.0 m, accessible to both grasses and trees) and lower layers (accessible only to trees). The plotted scenarios are the ones at the optimum depths (1.75 m for clay loam, 2.0 m for sandy loam, 2.25 m for sand). First, for all soil layers, less water is left in storage in September for ERD1 PC as compared to ERD1 C (compare with Figure 7a). Second, for the fine-textured soils (clay), a higher proportion of water is stored in the upper layers than in the lower layers, and trees have therefore lost the competitive advantage from water resource partitioning. More transpiration is attributed to grasses. For example, for clay loam at the optimum rooting depth (2.0 m with CF = 0.5, ERD1 PC) transpiration is partitioned into 30% grass and 70% tree transpiration (compare with Figure 11b). For the same case and CF =

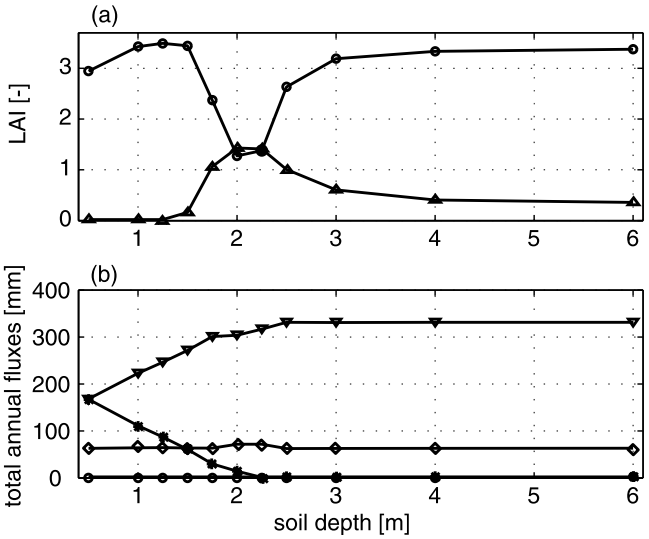

Figure 9. Predicted conditions at the end of a 500-a simulation with reduced khareef cloud cover (scenario ERD1 PC) for sandy loam and varying soil depth. (a) LAI for upper (deciduous trees, triangles) and lower (C4 grass, circles) canopy and (b) corresponding water budget for the same case, expressed in annual fluxes: transpiration (triangles), drainage (asterisks), evaporation (diamonds), and surface runoff (circles).

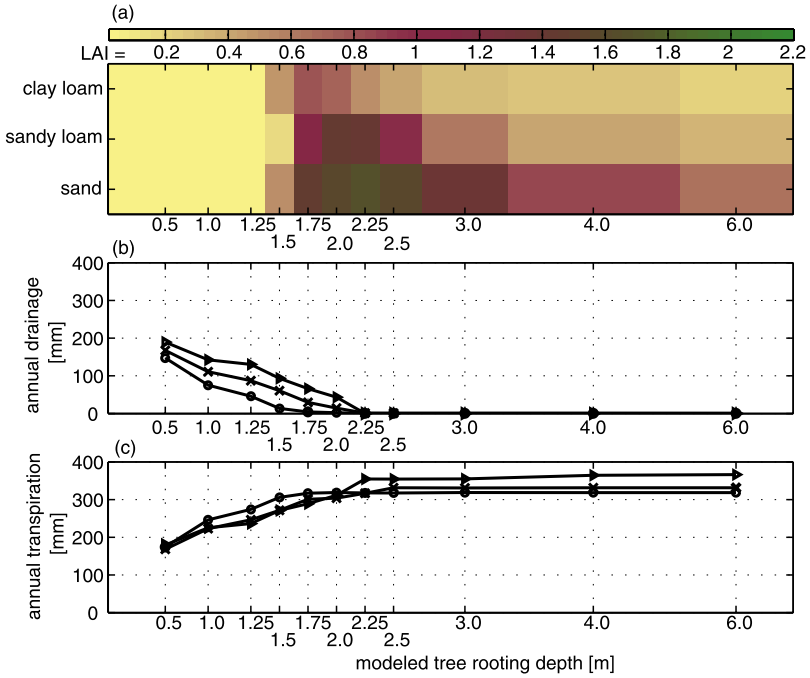

Figure 10. Overview over predicted conditions at the end of a 500-a simulation with reduced khareef cloud cover (scenario ERD1 PC). (a) Predicted LAI of the upper canopy (deciduous trees), (b) corresponding total annual drainage, and (c) corresponding total annual transpiration. Soil types are sand (circles), sandy loam (crosses), and clay loam (triangles).

0.5 (ERD1 C), the optimum depth was 2.75 m, and the transpiration was almost entirely (97%) attributed to trees (Figure 11a). Modeled LAI for the upper canopy was 1.43 and 2.02 for the partially cloudy (ERD1 PC) and cloudy (ERD1 C) scenarios. The difference in direct soil evaporation was negligible (15 mm). The same pattern holds for the other soil types, but the effect is more pronounced in fine soils than in coarse soils.

7. Discussion and Conclusion

[40] With a dynamical vegetation model we investigated the dependence of a seasonal deciduous forest in Oman on cloud immersion for decreasing incoming radiation and evaporative demand during the summer wet season. When the model was forced with measured meteorological input and expected cloud cover it reproduced the observed vegetation (deciduous broadleaf trees with a herbaceous sublayer) and hydrologic dynamics well [*Hildebrandt et al.*, 2007]. On the contrary, when the cloud cover was reduced, the modeled vegetation at equilibrium was no longer trees, but C4 grasses. The model simulation suggests that the radiative shielding of the cloud cover plays an important role in making more water available for tree transpiration and productivity. With the cloud cover present, little energy is available for evapotranspiration during the wet season, and the received water infiltrates and fills the deep soil storage. This water is used up after the 3-month-long wet season and lasts for another 3 months into the dry season, thus doubling the length of the growing season for deep-rooted plants.

[41] This scenario also underscores that the forests in Dhofar thrive in an environment that is only marginally suited for them, thanks to the favorable seasonality of the cloud cover. The forests in Dhofar represent one case where forests seem to survive in a marginal climate. Similar sites appear to exist in other parts of the world. For example, the most arid FluxNet site in Yatir forest (Israel) [*Baldocchi et al.*, 2004; *Grunzweig et al.*, 2003] is also a pine plantation and surrounded by sparse shrub land. The climate is

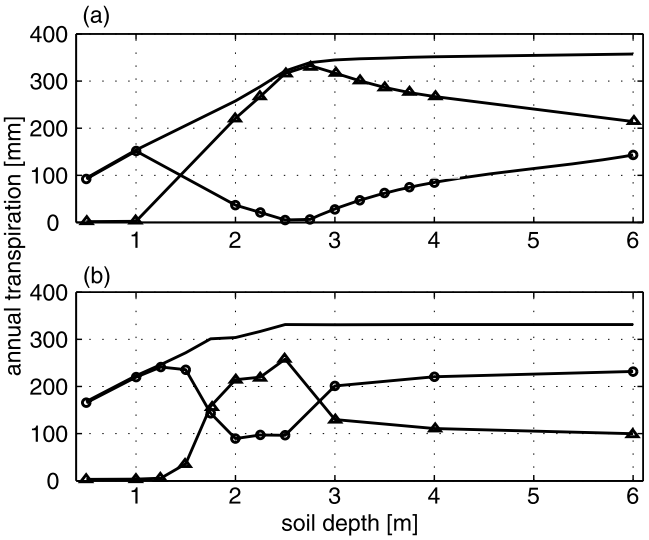

Figure 11. Partitioning of total transpiration (solid line) into upper (triangles) and lower (circles) canopy at different soil depths for free draining sandy loam: (a) cloudy khareef (scenario ERD1 C) and (b) partly cloudy khareef (scenario ERD1 PC).

comparatively arid (annual rainfall is 270 mm, with a ratio of rainfall to potential evaporation of 0.15 [*Grunzweig et al.*, 2003]), but of Mediterranean type. Not only is it noteworthy that the afforestation effort was successful in such a dry environment, and currently without irrigation, but also carbon assimilation rates are positive in this 35-a-old forest, and comparable to the temperate FluxNet sites. Clearly, the forest is well established and still growing, regardless of the dryness. The latter study concluded that much more land might be suitable for tree growth than suggested by currently used climate vegetation charts.

[42] With a sensitivity study using IBIS we showed that a characteristic rooting depth corresponds to maximum performance of trees in this environment. The characteristic depth was located at the shortest rooting depths for which transpiration is maximized, and the sum of all other losses was minimized. This was true for both lower boundary conditions, free drainage and impermeable rock (no drainage). In the free drainage scenario tree LAIs were maximized when drainage was approximately zero. In the case where no drainage was assumed, highest tree LAIs were predicted when surface runoff became zero, however in the latter case the negative effects of water logging are ignored for prediction of LAI. In both cases LAIs decreased when rooting depths were further increased beyond the optimum level. The latter behavior is a result of the assumption made regarding the uptake profile, but it reflects that it is efficient for trees to keep roots as short as possible [*Schenk and Jackson*, 2002b]. Our results imply that drainage should be close to zero under water-limited conditions, which is in agreement with observations for water-limited ecosystems [*Noy-Meir*, 1973], including cloud-affected ones [*Hutley et al.*, 1997]. The modeled optimum rooting depths depend on the soil type with coarse soils leading to deeper optimum rooting depths and higher tree LAI than fine soils. For all modeled soils, the optimum rooting depths for trees was much deeper than characteristic rooting depths for grasses (about 1 m). Tree LAI at optimum depth depended on the water storage in the deep soil (outside the reach of grasses), and not on the water storage in the entire soil column. Therefore in this environment the Walter hypothesis of resource partitioning seems to be valid, and facilitated by the cloud cover.

[43] Furthermore, we showed that for decreased cloud cover (implying increased evaporative demand during the filling of the soil storage) the optimum rooting depths moved upward. As a result, the partition size of the soil storage, which is reserved to trees, was decreased and trees were forced to compete with grasses in shallower layers. Tree LAIs at the optimum rooting depth were consequently lower for reduced cloud cover as compared to dense cloud cover. Cloud cover not only increased transpiration but also shifted the dominant driver of transpiration from grasses to trees. In other words, resource partitioning between trees and grasses (e.g., exclusion of grasses from access to deep layers for water uptake) is enhanced by persistent cloud cover.

[44] Our results are in good qualitative agreement with observations. *Wan et al.* [2002] observed that seasonality of water availability had an influence on rooting depth for snakeweed (*Gutierrezia sarothrae*). They found that snakeweed developed shallow root systems when it was irrigated during spring to summer, whereas it developed deeper roots when irrigated in winter. Similarly, *Schenk and Jackson* [2002b] concluded from analysis of a database of root patterns that rooting depth for perennial woody shrubs were deeper in winter precipitation systems than in summer precipitation systems. In winter precipitation systems the evaporative demand is lower than in summer precipitation systems, which is analogous to comparing a situation with cloudy and partly cloudy monsoon done here. The optimum rooting depths moved upward when evaporative demand increased. *Schenk and Jackson* [2002b] did not make the same observation for trees, which may however be related to the fact that some trees tap groundwater, which makes their rooting depth independent of soil moisture. At any rate, *Schenk and Jackson* [2002b, p. 480] concluded "Walters two-layer model of resources partitioning seems to be most appropriate in drier regimes (<500 mm annual precipitation) and systems with substantial winter precipitation." Our study suggests that the low evaporative demand and reduced temperatures, which are provided by the cloud cover during the moist season [*Hildebrandt et al.*, 2007], render the climate similar to a system with "substantial winter precipitation." Additionally, resource partitioning could be an important mechanism supporting survival of deep-rooted plants in Dhofar.

[45] Furthermore, coarse soils (here sand) had a larger amount of water stored in deeper layers than in shallow layers, even under conditions of higher evaporative demand (50% cloud cover). As a result, more water is available exclusively to trees than to grasses, and tree LAIs increased when the soil became coarser. This result is in agreement with *Noy-Meir*'s [1973] observation that coarser soils support denser and taller perennial vegetation than finer ones. Moreover, *Schenk and Jackson* [2002a] predicted from investigation of a large databases of root profiles that coarse soils were more likely to support deep rooted plants than finer soils. Similarly, *Hacke et al.* [2000] report substantially deeper roots for *Pinus tadea* in sand soils compared to loam.

[46] Our results are also in agreement with recent modeling studies using nonuniform root distributions. Results obtained by *Laio et al.* [2006] using an analytical model to determine root distributions of plant communities depending on climate and soil properties support deeper roots in coarser soils. *Collins and Bras* [2007] used a 1-D numerical ecohydrological model, where root profile was described by *Schenk and Jackson*'s [2002a] linear dose response model. When optimizing root profiles with regard to transpiration, they found that coarse soils lead to deeper roots than fine ones, and winter precipitation also favors deeper roots. Furthermore, deeper roots were found in environments where precipitation occurred mainly during times of low potential evaporation.

[47] For this investigation we had a limited time series of 2 a available (2003 and 2004). We used data collected only during 2004 to predict average conditions, since data from a nearby climate station suggested that 2003 was a year with exceptionally short monsoon and little precipitation. On the other hand, 2004 was a year with a monsoon of average length, although with slightly less rainfall [*Hildebrandt et al.*, 2007]. By using data from 2004, we may have assumed somewhat drier conditions for our model than in reality. We were also not able to consider the influence of climate

variability on the vegetation. This issue should be investigated as soon as longer time series become available. Finally, we enhanced net precipitation to account for stemflow as a point source leading to higher soil moisture around tree stems. This assumption leads to somewhat wetter conditions and allows for deeper infiltration. The model results for the role of tree grass competition are not affected by this assumption; rather, the key difference is that optimum rooting depths are deeper under the assumed moist conditions and tree LAIs are increased.

[48] For this analysis we used IBIS without adjusting any physiological parameters of the modeled vegetation. This mainly stemmed from the lack of information on vegetation parameters in this relatively undocumented area. We find it even more remarkable that IBIS was able to reproduce the vegetation dynamics in Dhofar, although the vegetation is parameterized in broadly defined plant functional types. However, our analysis of rooting depth shows how the sensitive parameterization of the rooting profile affects modeled transpiration and net primary productivity, which is consistent with analysis done elsewhere [*Feddes et al.*, 2001; *Hallgren and Pitman*, 2000; *Kleidon and Heimann*, 1998]. More work is needed to account for changing rooting behavior of the same plant functional types in different environments within SVAT schemes.

[49] On the basis of our mathematical modeling experiments, we highlight the potential role of cloud cover in increasing transpiration as well as creating an environment that favors the growth of deep-rooted plants. Without the cloud cover, tree vegetation in this region would not be expected. The cloud cover might therefore create an ecological niche for forest growth in this region. More experimental work on below-groundwater use is necessary to test these modeling results. Ecosystems that depend on regular cloud immersion have been defined as cloud forests. In the companion paper [*Hildebrandt et al.*, 2007] we proposed, on the basis of field observations, that the forests of Dhofar are cloud forests, for their existence is strictly linked to cloud immersion during the summer moist season. The modeling study presented here supports these results, and provides more insight into a rarely studied area and fragile ecosystem of high importance for biodiversity on the Arabian Peninsula [*Miller*, 1994].

[50] **Acknowledgments.** We thank Amilcare Porporato, Andrew Guswa, and four anonymous reviewers for providing us with detailed comments and help improving the manuscript. We also thank Daniel Collins for his comments on the manuscript. Financial support for this research was provided by a grant from the Ministry of Regional Municipalities, Environment and Water Resources of the Sultanate of Oman and by a fellowship from the Martin Society of Fellows for Sustainability.

References

Baldocchi, D. D., L. K. Xu, and N. Kiang (2004), How plant functional-type, weather, seasonal drought, and soil physical properties alter water and energy fluxes of an oak-grass savanna and an annual grassland, *Agric. For. Meteorol.*, *123*, 13–39.

Brook, G. A., and S.-W. Shen (2000), Rainfall in Oman and the United Arab Emirates: Cyclicity, influence of the Southern Oscillation and what the future may hold, *Arab World Geogr.*, *3*, 78–96.

Brown, J. H., T. J. Valone, and C. T. Curtain (1997), Reorganization of an arid ecosystem in response to recent climate change, *Proc. Natl. Acad. Sci. U. S. A.*, *94*, 9729–9733.

Collins, D. B. G., and R. L. Bras (2007), Plant rooting strategies in water-limited ecosystems, *Water Resour. Res.*, *43*, W06407, doi:10.1029/2006WR005541.

Ehleringer, J. R., S. L. Phillips, W. S. F. Schuster, and D. R. Sandquist (1991), Differential utilization of summer rains by desert plants, *Oecologia*, *88*, 430–434.

Feddes, R. A., et al. (2001), Modeling root water uptake in hydrological and climate models, *Bull. Am. Meteorol. Soc.*, *82*, 2797–2809.

Foley, J. A., I. C. Prentice, N. Ramankutty, S. Levis, D. Pollard, S. Sitch, and A. Haxeltine (1996), An integrated biosphere model of land surface processes, terrestrial carbon balance, and vegetation dynamics, *Global Biogeochem. Cycles*, *10*, 603–628.

Gale, M. R., and D. F. Grigal (1987), Vertical root distributions of northern tree species in relation to successional status, *Can. J. For. Res.*, *17*, 829–834.

Green, S. R., and B. E. Clothier (1995), Root water-uptake by kiwifruit vines following partial wetting of the root-zone, *Plant Soil*, *173*, 317–328.

Grunzweig, J. M., T. Lin, E. Rotenberg, A. Schwartz, and D. Yakir (2003), Carbon sequestration in arid-land forest, *Global Change Biol.*, *9*, 791–799.

Hacke, U. G., J. S. Sperry, B. E. Ewers, D. S. Ellsworth, K. V. R. Schafer, and R. Oren (2000), Influence of soil porosity on water use in Pinus taeda, *Oecologia*, *124*, 495–505.

Hallgren, W. S., and A. J. Pitman (2000), The uncertainty in simulations by a global biome model (BIOMES) to alternative parameter values, *Global Change Biol.*, *6*, 483–495.

Hildebrandt, A., M. Al Aufi, M. Amerjeed, M. Shammas, and E. A. B. Eltahir (2007), Ecohydrology of a seasonal cloud forest in Dhofar: 1. Field experiment, *Water Resour. Res.*, *43*, W10411, doi:10.1029/2006WR005261.

Holdridge, L. R. (1947), Determination of world plant formations from simple climatic data, *Science*, *105*, 367–368.

Hutley, L. B., D. Doley, D. J. Yates, and A. Boonsaner (1997), Water balance of an Australian subtropical rainforest at altitude: The ecological and physiological significance of intercepted cloud and fog, *Aust. J. Bot.*, *45*, 311–329.

Jackson, R. B., J. Canadell, J. R. Ehleringer, H. A. Mooney, O. E. Sala, and E. D. Schulze (1996), A global analysis of root distributions for terrestrial biomes, *Oecologia*, *108*, 389–411.

Jackson, R. B., H. A. Mooney, and E. D. Schulze (1997), A global budget for fine root biomass, surface area, and nutrient contents, *Proc. Natl. Acad. Sci. U. S. A.*, *94*, 7362–7366.

Kleidon, A., and M. Heimann (1998), A method of determining rooting depth from a terrestrial biosphere model and its impacts on the global water and carbon cycle, *Global Change Biol.*, *4*, 275–286.

Kucharik, C. J., J. A. Foley, C. Delire, V. A. Fisher, M. T. Coe, J. D. Lenters, C. Young-Molling, N. Ramankutty, J. M. Norman, and S. T. Gower (2000), Testing the performance of a dynamic global ecosystem model: Water balance, carbon balance, and vegetation structure, *Global Biogeochem. Cycles*, *14*, 795–826.

Lai, C. T., and G. Katul (2000), The dynamic role of root-water uptake in coupling potential to actual transpiration, *Adv. Water Resour.*, *23*, 427–439.

Laio, F., P. D'Odorico, and L. Ridolfi (2006), An analytical model to relate the vertical root distribution to climate and soil properties, *Geophys. Res. Lett.*, *33*, L18401, doi:10.1029/2006GL027331.

Lehmann, J. (2003), Subsoil root activity in tree-based cropping systems, *Plant Soil*, *255*, 319–331.

Li, K. Y., M. T. Coe, and N. Ramankutty (2005), Investigation of hydrological variability in West Africa using land surface models, *J. Clim.*, *18*, 3173–3188.

Li, Y., M. Fuchs, S. Cohen, Y. Cohen, and R. Wallach (2002), Water uptake profile response of corn to soil moisture depletion, *Plant Cell Environ.*, *25*, 491–500.

Lieth, H., and R. H. Whittaker (1975), *Primary Productivity of the Biosphere*, Springer, New York.

Miller, G. M. (1994), CPD site SWA 1. Dhofar fog oasis. Oman and Yemen, in *Centres of Plant Diversity: A Guide and Strategy for Their Conservation*, vol. 1, *Europe, Africa, South West Asia and the Middle East*, edited by V. H. Heywood and S. D. Davis, pp. 309–311, World Conserv. Union, Cambridge, U. K.

Noy-Meir, I. (1973), Desert ecosystems: Environment and producers, *Annu. Rev. Ecol. Syst.*, *4*, 25–51.

Pressland, A. J. (1976), Soil moisture redistribution as affected by throughfall and stemflow in an arid zone shrub community, *Aust. J. Bot.*, *24*, 614–649.

Romero-Saltos, H., L. Sternberg, M. Z. Moreira, and D. C. Nepstad (2005), Rainfall exclusion in an eastern Amazonian forest alters soil water movement and depth of water uptake, *Am. J. Bot.*, *92*, 443–455.

Sakuratani, T., T. Aoe, and H. Higuchi (1999), Reverse flow in roots of Sesbania rostrata measured using the constant power heat balance method, *Plant Cell Environ.*, *22*, 1153–1160.

Sala, O. E., R. A. Golluscio, W. K. Lauenroth, and A. Soriano (1989), Resource partitioning between shrubs and grasses in the Patagonian steppe, *Oecologia*, *81*, 501–505.

Schenk, H. J., and R. B. Jackson (2002a), The global biogeography of roots, *Ecol. Monogr.*, *72*, 311–328.

Schenk, H. J., and R. B. Jackson (2002b), Rooting depths, lateral root spreads and below-ground/above-ground allometries of plants in water-limited ecosystems, *J. Ecol.*, *90*, 480–494.

Schenk, H. J., and R. B. Jackson (2005), Mapping the global distribution of deep roots in relation to climate and soil characteristics, *Geoderma*, *126*, 129–140.

Scholes, R. H., and B. H. Walker (1993), *An African Savanna, Synthesis of the Nylsvley Study*, Cambridge Univ. Press, New York.

Schwinning, S., K. Davis, L. Richardson, and J. R. Ehleringer (2002), Deuterium enriched irrigation indicates different forms of rain use in shrub/grass species of the Colorado plateau, *Oecologia*, *130*, 345–355.

Schwinning, S., B. I. Starr, and J. R. Ehleringer (2005), Summer and winter drought in a cold desert ecosystem (Colorado plateau) part I: Effects on soil water and plant water uptake, *J. Arid. Environ.*, *60*, 547–566.

Stephenson, N. L. (1990), Climatic control of vegetation distribution: The role of the water balance, *Am. Nat.*, *135*, 649–670.

Walter, H. (1962), *Die Vegetation der Erde in oekophysiologischer Betrachtung. I. Die tropischen und subtropischen Zonen*, Fischer, Stuttgart, Germany.

Wan, C. G., I. Yilmaz, and R. E. Sosebee (2002), Seasonal soil-water availability influences snakeweed, root dynamics, *J. Arid. Environ.*, *51*, 255–264.

Wang, E. L., and C. J. Smith (2004), Modelling the growth and water uptake function of plant root systems: A review, *Aust. J. Agric. Res.*, *55*, 501–523.

Whittaker, R. H. (1975), *Communities and Ecosystems*, MacMillan, New York.

Williams, C. A., and J. D. Albertson (2004), Soil moisture controls on canopy-scale water and carbon fluxes in an African savanna, *Water Resour. Res.*, *40*, W09302, doi:10.1029/2004WR003208.

E. A. B. Eltahir, Department for Civil and Environmental Engineering, Massachusetts Institute of Technology, Cambridge, MA 02139, USA.

A. Hildebrandt, UFZ Helmholtz Centre for Environmental Research, Permosestr. 15, Leipzig D-04318, Germany. (hildebra@alum.mit.edu)